Interface Focus

rsfs.royalsocietypublishing.org

Review

Cite this article: Fadeeva E, Deiwick A, Chichkov B, Schlie-Wolter S. 2014 Impact of laser-structured biomaterial interfaces on guided cell responses. *Interface Focus* **4**: 20130048.
http://dx.doi.org/10.1098/rsfs.2013.0048

One contribution of 10 to a Theme Issue 'Nano-engineered bioactive interfaces'.

Subject Areas:
biomaterials, biomedical engineering, nanotechnology

Keywords:
ultrashort pulse laser structuring, nano- and microsized surface topographies, biomaterial–cell interactions, selective cell control

Author for correspondence:
Sabrina Schlie-Wolter
e-mail: s.schlie@lzh.de

Impact of laser-structured biomaterial interfaces on guided cell responses

Elena Fadeeva[1], Andrea Deiwick[1], Boris Chichkov[1,2] and Sabrina Schlie-Wolter[1,2]

[1]Laser Zentrum Hannover e.V., Hollerithallee 8, 30419 Hannover, Germany
[2]Institute of Quantum Optics, Leibniz University Hannover, Welfengarten 1, 30167 Hannover, Germany

To achieve a perfect integration of biomaterials into the body, tissue formation in contact with the interface has to be controlled. In this connection, a selective cell control is required: fibrotic encapsulation has to be inhibited, while tissue guidance has to be stimulated. As conventional biomaterials do not fulfil this specification, functionalization of the biointerface is under development to mimic the natural environment of the cells. One approach focuses on the fabrication of defined surface topographies. Thereby, ultrashort pulse laser ablation is very beneficial, owing to a large variety of fabricated structures, reduced heat-affected zones, high precision and reproducibility. We demonstrate that nanostructures in platinum and microstructures in silicon selectively control cell behaviour: inhibiting fibroblasts, while stimulating neuronal attachment and differentiation. However, the control of fibroblasts strongly correlates with the created size dimensions of the surface structures. These findings suggest favourable biomaterial interfaces for electronic devices. The mechanisms which are responsible for selective cell control are poorly understood. To give an insight, cell behaviour in dependence of biomaterial interfaces is discussed—including basic research on the role of the extracellular matrix. This knowledge is essential to understand such specific cell responses and to optimize biomaterial interfaces for future biomedical applications.

1. Introduction

To replace damaged tissue or support dysfunctions within the tissue, alloplastic materials are introduced into the organism. These biomaterials should not only imitate the mechanical and structural properties of the tissue that needs to be substituted, but also defined cell responses have to be addressed in order to guide tissue formation in contact with the biomaterial and by this means support implant functions. As the tissues within the human body are very diverse with respect to their composition and functionality, for each biomedical application a specific biomaterial has to be selected. The implantation procedure as well as the presence of a biomaterial within the body always cause a biological reaction [1,2]. In all cases, a high biocompatibility of the biomaterial is required to stimulate appropriate host tissue responses. However, cascades of wound healing right after implantation and inflammatory reactions in general even after contact times of years can reduce a material's biocompatibility and harm the patient. Inflammation is characterized by complex signalling cascades, which finally result in the formation of fibroblastic scar tissue surrounding the implanted material. As a consequence, the implant gets isolated from its supporting tissue and fails. The extent and time duration of inflammation strongly correlate with the material properties, composition, size and geometry. To overcome problems related to inflammation, the biocompatibility of materials has to be enhanced in a way that the attachment and proliferation of fibroblasts, which form the scar tissue, have to be inhibited, while the other cells should not be negatively affected or even be stimulated. Interference in this cell competition is defined as a selective cell control—one of the big challenges in biomedical research and a strongly demanded property of innovative biomaterials. For instance, the functionality

Royal Society Publishing

of electronic devices could be improved by using materials offering this specific cell control: as fibroblasts attach on the electrodes, no close connection to neuronal cells is possible. Therefore, the quality of electric signals is limited.

Owing to the technical requirements of the biomaterial, it is difficult to find alternatives for the commonly used basis material. Therefore, research has turned to manipulating the biomaterial surface. Several functionalization approaches have been performed in order to create a biomaterial interface, which is biologically inspired and copies the natural environment of the cells. This environment *in vivo* is actually pretty well defined. Cells are always embedded in a tissue-specific extracellular matrix (ECM), which basically consists of soluble molecules, glycosaminoglycans, proteoglycans and adhesive proteins to anchorage cells [3,4]. Besides the structural support, cell binding to the ECM stimulates outside-in signalling cascades needed for survival, cell cycle progression and differentiation [5]. In a biochemical functionalization approach, the chemical composition of the material surface mimics the ECM or components or binding fragments of the ECM are bound to the biomaterial interface directly. Via a physical functionalization approach, the elasticity, charge or topographical aspects of the ECM are copied.

In past decades, it was demonstrated that cells are very sensitive to the topographical information of their environment being able to respond to objects as small as 5 nm [6]. In this connection, defined surface topographies were shown to guide selectively cell responses. Surface roughness and specific surface features at nano- and micrometre scales were able to affect cell orientation, morphology, proliferation and differentiation [7–10]. For the production of such topographies, different technologies, such as lithography, polymer demixing, plasma treatment, etching and others, have been used. Thereby, the generation of surface features that vary in their composition, size and periodicity is still very challenging. Laser processing of biomaterials has several advantages over other methods, namely low surface contamination, low mechanical damage and controllable surface structuring of three-dimensional components with complicated geometries [11,12]. Owing to extremely short laser–material interaction times, femtosecond laser processing has additional advantages over long-pulse laser processing, namely a higher quality of machined structures, negligible material damage and strongly reduced heat-affected zones [13]. Various surface topographies at micro- and nanometre scales can be fabricated in almost all solid materials in a controllable, flexible and reproducible manner [14–16]. Via changing the laser-processing parameters, the size dimensions of each structure type can additionally be varied [14,17]. In summary, femtosecond laser material ablation enables the precise design of surface topographies, and therefore offers a platform to study systematically cell and tissue interactions with a defined topographical environment.

With respect to the optimization of biomaterial interfaces for neuronal electronic devices, it was analysed whether topographical functionalization via femtosecond lasers is able to control fibroblasts versus neuronal cells. An inhibition of fibrotic capsule formation is demanded in order to enhance the device performance, which simultaneously depends on a good attachment of neuronal cells followed by their neuronal differentiation. In the past, the selective stimulation of neuronal cells was often based on a reduced size of the electrodes. However, this could negatively affect the stimulating current density, corrosion and others. Besides a topographical impact on selective cell control, surface structuring could therefore also provide technical advantages, namely the improvement of the electrochemical properties owing to an increased surface area. We demonstrate that nano- and microscaled surface features in platinum (Pt) and silicon selectively inhibit fibroblasts but stimulate neuronal cells—making this surface functionalization very attractive for applications in biomedicine. However, the control over fibroblasts strongly correlates with the size dimension of the topography. For a better understanding of the results, cell interactions with biomaterial interfaces are additionally discussed.

2. Material and methods

2.1. Surface structuring

Commercially available Pt foils with a purity of 99.99% and p-type silicon 110 (Si) (Goodfellow, Bad Nauheim, Germany) were cleaned with acetone followed by methanol, and finally rinsed in distilled water in an ultrasonic bath. Surface structuring on $1 \times 1\ mm^2$ was realized via material ablation using an amplified Ti : sapphire femtosecond laser system (Femtopower Compact Pro, Femtolasers Production GmbH, Vienna, Austria). This system delivers linearly polarized sub-30 fs pulses at 800 nm at a repetition rate of 1 kHz. Both surface features were generated by raster scanning the laser beam across the samples. For nanostructures in Pt, a laser fluence of $7.7\ J\ cm^{-2}$ was used; for microsized spike structures, the laser fluence was varied between 0.36 and $3.6\ J\ cm^{-2}$ in order to control the spike height and periodicity. Pt samples were processed under normal atmospheric conditions, whereas silicon samples were processed in SF_6 process gas (500 Torr). After structuring the Pt, the samples were cleaned in acetone using an ultrasonic bath; the silicon samples were cleaned using 10% hydrofluoric acid aqueous solution and rinsed in distilled water. The structured samples were visualized with a scanning electron microscope. Further analysis of the material and structuring properties can be found elsewhere [14–16,18]. Before cell culture experiments, Pt nanostructures and Si microsized spike structures were sterilized under UV light for 30 min. Unstructured Pt and Si samples always served as controls.

2.2. Cell culture

In contrast to primary cells, which are hardly available—especially human neuronal cells—cell lines are a reliable cell model for *in vitro* studies. To overcome interspecies differences, we used human foreskin HFF-1 fibroblasts and human SH-SY5Y neuroblastoma cells. Rat pheochromocytoma PC-12 cells are an acceptable cell model to study neuronal differentiation, because they exhibit typical neuronal markers after treatment with nerve growth factor (NGF). All cell lines were purchased from DSMZ (Braunschweig, Germany) and the culture media from Lonza (Basel, Switzerland); other reagents were purchased from Sigma-Aldrich (Taufkirchen, Germany). Fibroblasts and neuroblastoma cells were cultured in Dulbecco's modified Eagle's medium F-12 supplemented with 10% fetal bovine serum (FCS, Biochrom, Berlin, Germany) and antibiotics. For the cultivation of PC-12 cells, RPMI medium with additional 10% horse, 5% FCS and antibiotics was used [18]. To induce a neuronal differentiation of PC-12 cells, $100\ \mu g\ ml^{-1}$ NGF was added. Undifferentiated control PC-12 cells were cultured without NGF under the same conditions. As PC-12 cells are suspension cells, additional coating onto the substrate was required to induce cell attachment. For that purpose sterile coatings each of $5\ \mu g\ cm^{-2}$ laminin (LA; dissolved in phosphate-buffered saline, PBS), collagen type I (COL, dissolved in 0.02 N acetic acid), poly-D-lysine (PDL, dissolved in water) and a 1 : 1 combination of COL–PDL were compared [18]. After incubating

at 37°C for 1 h, the coated samples were washed with PBS and used for the cell studies. Uncoated samples served as a control. All cell lines were kept in a humidified cell incubator with 5% CO_2 at 37°C (Thermo Electron Cooperation, Bonn, Germany).

The cell density (cells ml^{-1}) was determined automatically using a Casy TT cell counter (Roche, Mannheim, Germany). In more detail, the adherent cells were trypsinized using a 0.025% trypsin-EDTA solution, which was incubated for 5–10 min at room temperature. Afterwards serum-containing cell culture medium was added. This cell suspension was collected and centrifuged at 500*g* for 10 min (Universal 320, Hettich, Düsseldorf, Germany). Finally, the pellet was dissolved in cell culture media with an appropriate volume and counted.

2.3. Cell proliferation

The growth behaviour of the cells was characterized by their doubling time. The doubling time is defined as the time needed to pass the cell cycle once. In the first place, the seeding cell density (cells ml^{-1}) was determined. After 48 and 96 h cultivation time, the adherent cell density was quantified as described earlier. The exponential growth curve could be quantified via $y = m^x\ b$, where y refers to the cell density (cells ml^{-1}) and x to the cultivation time (h). To figure out the doubling time of the cells, the double of the initial seeded cell density was fitted into the curve equation and the corresponding x-value for the cultivation time was calculated. The results are given as average (h) $\pm$s.e.m. of four independent measurements. For the proliferation studies in dependence of laser-structured materials, the following average cell densities were seeded out: 7.1×10^5 cells ml^{-1} fibroblasts and 5.5×10^6 cells ml^{-1} neuroblastoma cells.

2.4. Cell imaging: electron microscopy, morphology and neuronal differentiation

To visualize the localization of fibroblasts cultured on microsized Si spikes with different spike-to-spike distances, the samples were prepared for electron microscopy [17]. After 24 h cultivation time, the cells were fixed with 3% glutaraldehyde (dissolved in PBS) at room temperature for 15 min. After several washing steps with PBS, another fixation followed with 2% osmium tetroxide (dissolved in PBS). Then the samples were dehydrated through a series of different ethanol concentrations up to 100% for 10 min each. Before imaging, the samples were dried with a critical point dryer and sputter-coated with a 5 nm gold layer.

Cell morphology on the laser-structured Pt and Si samples was investigated with respect to the length of the cells (micrometres). After 24 h cultivation time, fibroblasts and neuroblastoma cells were fixed using 4% formaldehyde (dissolved in PBS) at 4°C for 20 min. Phalloidin-Atto 488 was used to stain actin filaments and Hoechst 33342 for nucleus staining. Both reagents were dissolved in 0.3% Triton X-100 PBS solution and given onto the samples at 37°C for 1 h. Finally, the samples were washed with PBS and conserved in PBS.

To analyse the topographical impact on neuronal differentiation, undifferentiated control PC-12 cells without NGF-containing medium and differentiated PC-12 cells with NGF-containing medium were cultured on nanostructured Pt for 48 h [18]. As described above, the influence of additional coatings with LA, COL, PDL and COL–PDL was further compared. The cells were fixed using 4% formaldehyde (dissolved in PBS) at 4°C for 20 min. Following several washing steps with PBS, 0.5% bovine serum was added to block unspecific antibody binding. Primary antibodies for beta III tubulin and focal adhesion kinase FAK p-Tyr^{397} were incubated at 4°C overnight. Beta III tubulin enables detection of dendrites, which are a typical characteristic of neuronal cells, while the component of focal adhesion complexes FAK identifies the attachment of the cells to the substrate via binding to integrin receptors. After further washing steps with PBS, the corresponding secondary antibodies and Hoechst 33342 for nucleus staining were added at 37°C for 1 h. Then the samples were washed again and conserved in PBS.

Images were recorded with a fluorescence microscope (Nikon, Düsseldorf, Germany). Concerning quantification of cell length, ImageJ software was applied (http://rsbweb.nih.gov/ij/). Using the task straight line selection, a line was placed on the length of the entire cell body. Automatically, the pixel length for the line was created, which was then transferred to micrometre scale. The results are given as the average of cell length (μm) $\pm$s.e.m. obtained from 50 independent cells per treatment.

2.5. Impact of extracellular matrix components

To achieve more basic knowledge about cell attachment, one of the key factors in biomaterial–cell interactions, the impact of the ECM components fibronectin (FIB) and LA, was analysed [4]. LA from Engelbreth-Holm-Swarm murine sarcoma basement membrane and FIB from bovine plasma were dissolved in 0.01% PBS; glass slides were coated with 2 μg cm^{-2} LA and 5 μg cm^{-2} FIB at room temperature for 30 min. All slides were washed with PBS afterwards and sterilized under UV light for 30 min. The responses of fibroblasts and neuroblastoma cells cultured on FIB- and LA-coated glass substrates was characterized with respect to the adhesion time T_{Ad} (min), cell morphology given as cell length (μm) and doubling time (h).

The adhesion time T_{Ad} characterizes the time needed until half of the seeded non-adherent cells attach to the material surface [19]. For each treatment, 10×10^4 cells ml^{-1} of fibroblasts and 10×10^5 cells ml^{-1} neuroblastoma cells were seeded out. Over a total cultivation time of 1 h, each 10 min the cell density (cells ml^{-1}) was counted as described earlier. However, no trypsination was necessary, because the cell number of non-attached cells was of interest. Therefore, the entire cell suspension including the non-adherent cells was simply collected. Quantification of T_{Ad} is based on the first-order reaction, taking its origin from chemical kinetics. A detailed derivation of the formula can be found in [19]. The results are presented as the average of T_{Ad} (min) $\pm$s.e.m. of four independent measurements.

For the proliferation study, an initial cell density of 6.2×10^4 cells ml^{-1} of fibroblasts and 5.8×10^4 cells ml^{-1} of neuroblastoma cells was seeded out. The doubling time (h) and cell length (μm) of the cells were determined as described earlier. In contrast to the previous description, T_{Ad} and morphology analyses were carried out under serum-free culture conditions. Moreover, cell morphology was detected after 5 h cultivation time instead of 24 h.

2.6. Statistical analysis

To analyse whether statistical differences between the control and laser-structured Pt and Si surfaces occurred and accordingly between the control and LA- or FIB-coated substrates, Student's t-test was applied with significance levels of $^*p < 0.05$, $^{**}p < 0.01$ and $^{***}p < 0.001$.

3. Results

3.1. Surface properties

On the one hand, laser processing of Pt generated a porous texturing with nano- and microscaled cavities and aggregates (figure 1*a*). On the other hand, laser ablation of Si resulted in microsized conical surface features called spikes, which were randomly orientated and quasi-periodical on the entire surface. By varying the laser fluence during the fabrication process, it was possible to control the average spike-to-spike distances from 2 to 15 μm [14,17,20]. Two

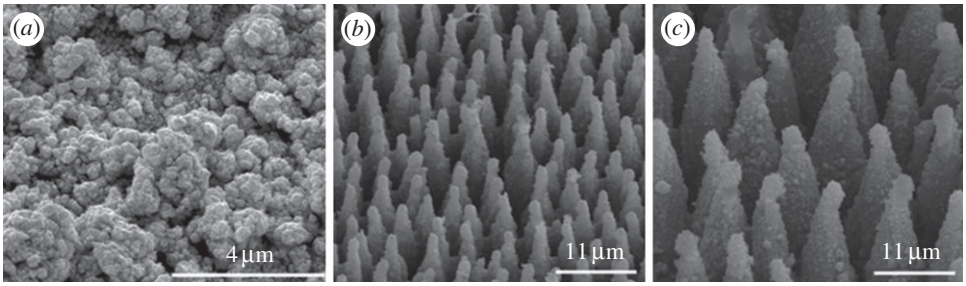

Figure 1. Scanning electron images of laser-generated surface topographies: (*a*) nanostructures in Pt; microsized spike structures in Si with (*b*) small and (*c*) large spike-to-spike distances.

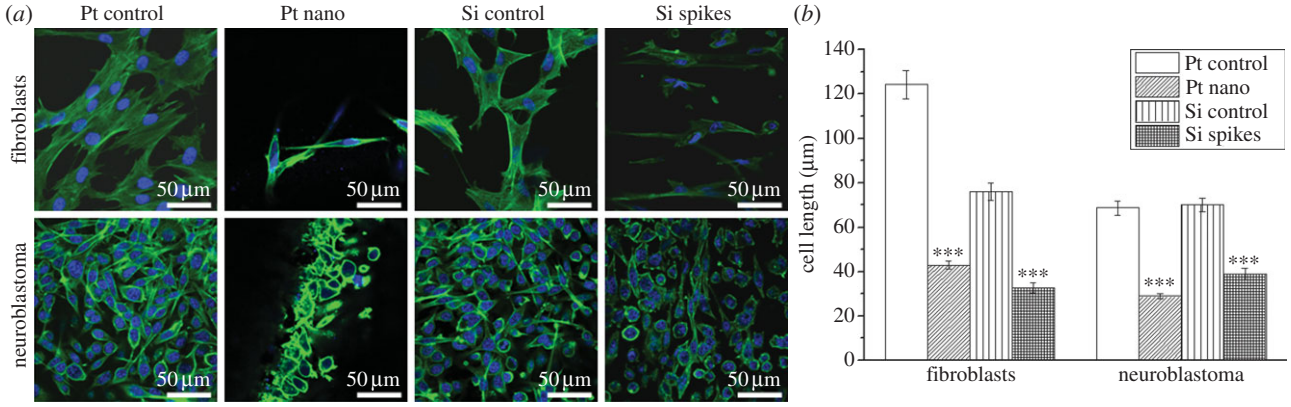

Figure 2. Analysis of cell morphology of fibroblasts and neuroblastoma cells in dependence of laser-generated surface topographies in Pt and Si after 24 h cultivation time. (*a*) Fluorescence images of actin filament-stained (green) and nucleus-stained (blue) cells, where actin is a component of the cytoskeleton. (*b*) Quantification of the cell length given as the average $\pm$ s.e.m. obtained from 50 cells per treatment. ***$p < 0.001$.

different size dimensions of Si spikes are exemplarily shown in figure 1*b*,*c*. For the comparison between fibroblasts and neuroblastoma cells average distances of 4.8 µm were used. To analyse fibroblasts' responses in dependence of the produced size dimensions of the topography, average spike-to-spike distances of about 2 µm and about 7 µm were compared.

In recent studies, we figured out that surface structuring can cause an increase in the water contact angle [14–16,20]. The contact angle of 62° of unstructured Si was increased to 130°, while the contact angle of 85° of unstructured Pt reached a value of 158° when nanostructured. Energy-dispersive X-ray (EDX) analysis pointed out that the chemical composition of the material was not changed during the fabrication process [14]. We also demonstrated that the produced surface features can additionally be coated without negatively affecting the texturing [18]. Measurements of impedance spectra revealed that nanostructuring reduces the impedance of Pt even when coated with COL, COL–PDL or LA [18].

3.2. Selective cell control of fibroblasts and neuroblastoma cells by nano- and microstructures

Other studies revealed that surface structuring did not induce cytotoxic effects [14,18]. Topographical impacts on cell behaviour were characterized via cell morphology and proliferation. The responses to nanostructured Pt and microstructured Si with spikes having an average spike-to-spike distance of 4.8 µm were compared. Figure 2*a* shows that on control surfaces fibroblasts had an elongated cell shape forming many cellular extensions. Neuroblastoma cells were either elongated or rounded on control surfaces. In line with the topography, fibroblasts changed their cellular shape. On nanostructured Pt more rounded cells were present, while on the microsized Si spike structures cells totally looked abnormal. On the contrary, no big differences in cell morphology between the control surface and nano- and microstructured surfaces for neuroblastoma cells were observed (figure 2*a*). However, there seemed to be fewer elongated cells on both topographies. To get more insights, cell length for all treatments was quantified after 24 h cultivation time (figure 2*b*). It could be confirmed that fibroblasts were significantly less spread on both texturing via reducing an average cell length of 124 µm on the Pt control to 42 µm on Pt nanostructures and from 75.84 µm on the Si control to 32 µm on Si spike structures. Neuroblastoma cells also reduced their average control length of 68 to 29 µm on Pt nanostructures and from 70.07 to 39 µm on Si spike structures. On both control surfaces fibroblasts showed an average doubling time of about 32 h, which was dramatically increased to 60 h on nanostructured Pt and even up to 91 h on spike-structured Si (figure 3). These results signified that fibroblasts proliferate a lot slower on the presented topographies. On the contrary, the proliferation of neuroblastoma cells was not negatively affected (figure 3). The average doubling times were similar on all investigated surfaces with reference to 69 h on the Pt control and 72 h on the Si control: 67 h on Pt nanostructures and 76 h on Si microstructures. In summary, these results pointed out a selective cell control between fibroblasts and neuroblastoma cells.

Whether the topographical influence on fibroblasts was dependent on the present size dimensions of the texturing was analysed with spike structures in Si having variable spike-to-spike distances (figure 4) [17]. On flat Si, fibroblasts were well spread and presented a normal cell shape. Moreover, the entire unstructured surface was totally covered with cells.

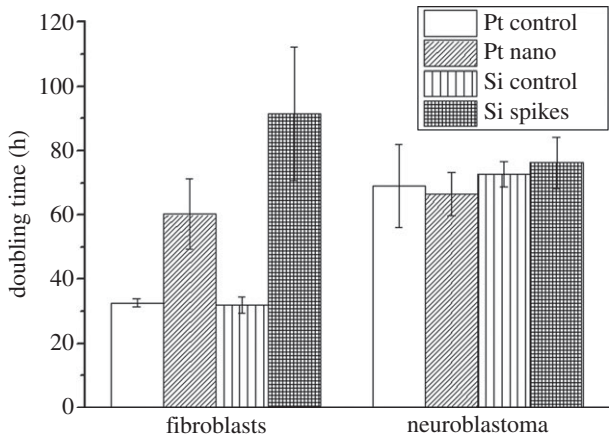

Figure 3. Proliferation of fibroblasts and neuroblastoma cells in dependence of the laser-generated surface topographies quantified by their doubling time. The results are presented as average $\pm$s.e.m. of four independent measurements.

On big spike-to-spike distances of 7 µm, the results were totally different (figure 4*a*): first, there were fewer cells attached on the structured surface; second, these results indicate that cell growth on the structures might be reduced; and third, fibroblasts were smaller and more rounded than on the unstructured Si. On small spike-to-spike distances of 2 µm no differences between the unstructured and structured surface occurred (figure 4*b*). Obviously, the inhibition of fibroblasts (figures 2 and 3) strongly correlates with the microsize dimensions of the topography.

3.3. Stimulation of neuronal attachment and differentiation of PC-12 cells on nanostructures

The impact of nanostructures in Pt on neuronal differentiation was investigated with PC-12 cells [18]. This cell line is a well-described model to study neuronal differentiation, owing to the expression of typical neuronal markers after the addition of NGF. Problematic is the fact that PC-12 cells are suspension cells—but cell attachment is a basic requirement for neuronal differentiation. To achieve an attachment of PC-12 cells, coatings of LA, COL, PDL or COL–PDL are required. Therefore, unstructured and structured Pt with additional coatings had to be compared; uncoated substrates served as the reference. On unstructured uncoated and unstructured LA-coated Pt, no cell attachment was possible (figure 5). They adhered on all other unstructured coatings and entirely on all structured coated surfaces. Interestingly, the cells were able to attach onto uncoated but structured Pt. This finding indicates that the presented topography itself significantly enhances the attachment of PC-12 cells, independent of the culturing conditions with or without NGF. It is confirmed by staining of FAK p-Tyr^{397}, a component of the focal adhesion complexes which is only expressed in cells that are bound via integrin receptors to the surface. In a recent study, the amount of FAK was further quantified. We found that it was most expressed when the surface was additionally coated with COL and COL–PDL [18]. Differentiation of the cells was verified by beta III tubulin, which is a component of dendrites (figure 5). In this connection, neuronal differentiation correlates with the formation of elongated cells having long dendrites, while failure of differentiation refers to rounded cells without dendrites. Undifferentiated cells were not able to form dendrites on all presented surfaces and coatings. Only under NGF-culturing conditions did differentiation take place. However, it strongly correlated with the surface design. The best differentiation via beta III tubulin occurred on coatings with COL and COL–PDL. Thereby, the best results were observed when the coating was combined with the nanostructures, indicating that the presented topography not only enhanced neuronal attachment, but also neuronal differentiation. Moreover, these results pointed out a strong correlation between the degree of attachment via FAK and degree of differentiation—as long as NGF was present. Without NGF a strong attachment was not sufficient to stimulate neuronal differentiation of PC-12 cells.

3.4. Laminin and fibronectin guide selectively the behaviour of fibroblasts and neuroblastoma cells

Attachment of cells is one of the key events in biomaterial–cell interactions. In this connection, the ECM plays a fundamental role, because it forms a linkage between the material surface and cells [4,5]. For this reason, basic knowledge on the functionality of the ECM is required. Therefore, the effects of the ECM components LA and FIB on fibroblasts and neuroblastoma cells were compared with respect to the adhesion time, morphology quantified by cell length after 5 h cultivation time and doubling time (table 1) [4]. Fibroblasts attached a lot faster to FIB with a T_{Ad} of 15.89 min than to LA with a T_{Ad} of 24.22 min. Neuroblastoma cells attached to LA and FIB in a comparable manner with T_{Ad} values of 16.89 min and 17.57 min, respectively. In comparison to the control surface, fibroblasts were less elongated on both ligands. The control cell length of about 122 µm was reduced to about 110 µm on FIB and even more reduced to about 99 µm on LA. Neuroblastoma cells were also less elongated on FIB with a cell length of about 25 µm when compared with the control of about 30 µm. However, these cells were significantly more elongated on LA with a value of about 54 µm. Fibroblasts proliferated slower on LA with a doubling time of about 40 h than on the control with a doubling time of about 32 h. But they grew a lot faster on FIB with a doubling time of about 25 h. This finding was opposite for neuroblastoma cells. The control doubling time of about 54 h was reduced to about 46 h on LA and increased to 65 h on FIB. All results demonstrated that the ECM selectively guides cell responses in a way such that fibroblasts responded better to FIB and neuroblastoma cells better to LA.

4. Discussion

Depending on the biomedical application, a biocompatible basis material is selected, which mimics the structural, mechanical and biochemical properties of the tissue that is supposed to be replaced. The critical parameter of the material is its surface, because it affects the interaction with cells [21]. Owing to problems of inflammatory reactions, there is a big demand and challenge to design biomaterial interfaces that inhibit the formation of fibrotic scar tissue, but stimulate the behaviour of cells, which promote biomaterial integration into the tissue, and thereby implant functions [1,2]. The usage of defined surface topographies, taking its origin from a physical material functionalization, is a possible approach to control selectively cell responses.

Femtosecond laser ablation was shown to be very attractive for a topographical functionalization of the biomaterial

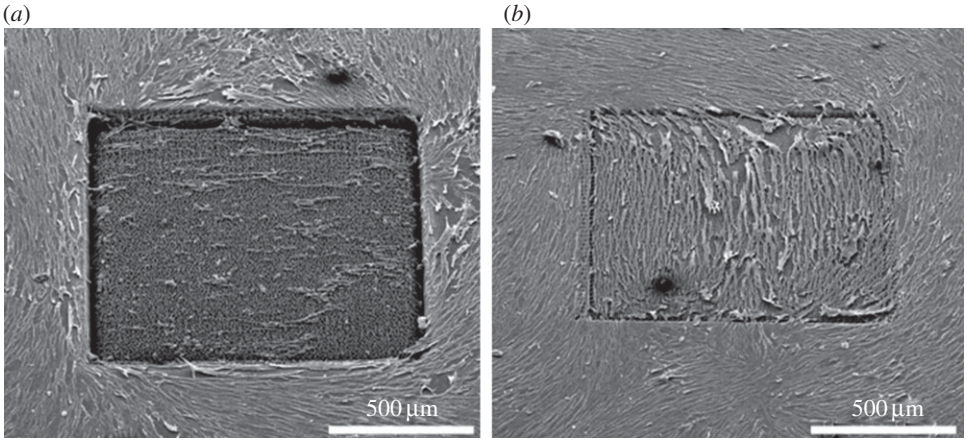

Figure 4. Scanning electron images of fibroblasts cultured on microsized Si spikes with different spike-to-spike distances after 24 h cultivation time: (*a*) average 7 µm spike-to-spike distances; (*b*) average 2 µm spike-to-spike distances.

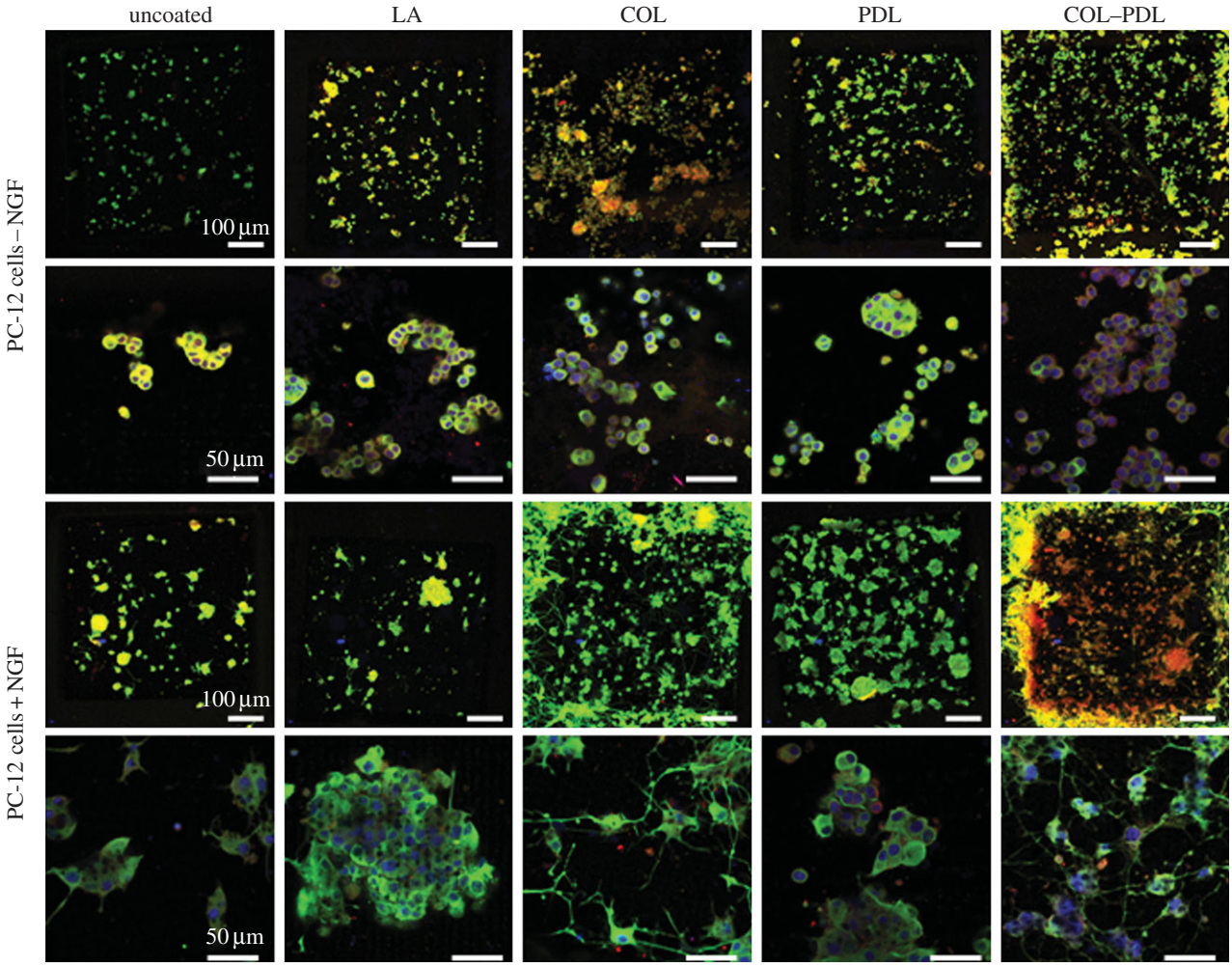

Figure 5. Analysis of the attachment and neuronal differentiation of PC-12 cells cultured on nanostructured Pt with additional coatings of LA, COL, PDL and COL–PDL after 48 h cultivation time. The control referred to an uncoated Pt substrate. Furthermore, the behaviour of undifferentiated cells (cultured in NGF-free medium) and differentiated cells (cultured in NGF-containing medium) was compared. Fluorescence images represent staining of beta III tubulin (green) as the main component of dendrites to visualize the degree of differentiation and FAK p-Tyr^{397} (red) to give insights into cell attachment, which is detectable via small dot-like features. The nuclei are further stained and located in the middle of each cell body.

interface with respect to its flexibility and high reproducibility [13]. We demonstrated that a large variety of surface texturing can be generated by this laser technology, such as a simple roughness, nanostructures (figure 1*a*), microsized groove structures, self-organized microsized spike structures (figure 1*b*,*c*) and a combination of nano- and microscales denoted as 'lotus' structures [10,14–18]. Tuning of the laser-processing parameters enabled a control of the size dimensions of each surface type. Moreover, the generated topographies can additionally be coated, without negatively affecting the texturing [18]. Basically, we have applied this manufacturing procedure for silicon, Pt and titanium, but structuring of polymers is also technically possible. EDX spectra revealed that laser structuring did not change the chemical composition of

Table 1. The impact of the ECM components LA and FIB on the behaviour of fibroblasts and neuroblastoma cells. Cell responses were quantified in terms of adhesion time T_{Ad} (min), cell morphology given as cell length (µm) and doubling time (h). The results are presented as average ±s.e.m. [4].

	T_{Ad} (min) ±s.e.m.		cell length (µm) ±s.e.m.				doubling time (h) ±s.e.m.			
	LA	FIB	control	LA	FIB		control	LA	FIB	
fibroblasts	24.22 ± 2.67	15.89 ± 1.33	121.55 ± 8.06	98.93 ± 7.07	110.62 ± 7.15		32.43 ± 5.08	40.35 ± 4.64	24.57 ± 0.94	
neuroblastoma	16.89 ± 1.99	17.57 ± 0.71	30.28 ± 2.24	53.93 ± 3.4***	25.03 ± 1.8		53.77 ± 4.77	46.12 ± 3.43	65.12 ± 9.02	

***$p < 0.001$.

the material [14]. In contrast to metals, structuring of polymers increased cytotoxic effects, which were caused by ablation debris and fragments that remained on the surface and could not be washed away [14,18]. Therefore, laser structuring of polymers is not recommended for biomedical applications. Alternatively, surface features in polymers can be generated via microreplication [22].

Wettability measurements revealed that surface structuring can cause a rise in the water contact angle in comparison with unstructured samples [14–16,20]. As variations of the materials' chemistry can be excluded, this rise is just an effect of the produced topography. According to the models of Wenzel and Cassie, structuring can result in a complete or incomplete wetting of the surface [23,24]. Even though the entire surface area is increased via structuring, in the case of incomplete wetting the surface area for contact is reduced—resulting in an increase in the water contact angle.

In order to selectively stimulate neuronal tissues, the size of stimulating electrodes should be reduced. This, in turn, requires stimulation with a higher current density [25]. As surface structuring increases the entire electrode surface area, we figured out whether nanostructuring of Pt, the material of choice for electronic devices, also affects material electrochemistry [18]. Usually, the effectiveness of Pt electrode surfaces has been enhanced via electrodeposition creating 'platinum black' electrodes, which present required low impedance spectra—but have a low biocompatibility [26,27]. Besides the fact that laser structuring increases the entire surface and does not cause cytotoxic effects [14,18], we found that structuring always reduced impedance values, even when the texturing was secondarily coated with LA, COL, etc. The achieved impedance spectra were similar to the properties of 'black platinum' [18]. Therefore, it can be concluded that surface structuring of Pt enables the production of technically improved Pt electrode surfaces.

For biomedical applications, functionalization techniques always have to be adapted to the *in vivo* situation. The potential of each material and interface design is characterized by cell *in vitro* testing in the first place. Recently, a lot of studies reported that cell behaviour can be influenced by surface topographies [6–9]. However, most of the research has been performed with one cell type, so that the impact on selective cell control has not been addressed. Here, we demonstrated that nanostructures in Pt and microsized spike structures in silicon are able to affect cell behaviour selectively. Cell morphology and proliferation of fibroblasts and neuroblastoma cells were specifically influenced (figures 2 and 3) [14,16,20]. We recently showed that this control correlated only with the texturing and not with the base material, such as silicon, silicone elastomer, Ormocomp or others [28]. Both cell types reduced their cell length in contact with the topography via adapting their cell shape to the texturing underneath. Additionally, both cell types were more rounded assuming influences on intracellular forces via their cytoskeleton. At the same time, the increased amount of rounded cells indicates poor attachment to the surface. They lack cellular extensions, which basically include focal adhesion complexes [19]. However, rounded cells may also indicate cell death or mitosis: the former can be excluded because the produced surfaces were not cytotoxic and the latter can be estimated via analysing cell proliferation. The proliferation of neuroblastoma cells was not negatively affected by the topographies, while fibroblasts dramatically

reduced their growth on both presented surface patterns. With respect to the morphology results, it can be assumed that neuroblastoma cells were more rounded because of cell growth, whereas fibroblasts were more rounded because of poor attachment. The selective influence on cell proliferation was also observed for 'lotus' structures in titanium, which inhibited the growth of fibroblasts but not the growth of human osteoblast-like cell line MG-63 [10,15].

As laser structuring offers the fabrication of one texturing type with variable size dimensions, we further analysed whether the inhibition of fibroblasts correlated with spike-to-spike distances in silicon. For average spike-to-spike distances bigger than 4.8 μm, the growth and morphology of fibroblasts were negatively affected, whereas average distances of about 2 μm were not problematic for these cells (figure 4). It can be concluded that not only the type of texturing, but also the size dimensions of each surface type have a specific impact on cells. Therefore, this surface parameter has to be taken into account for functionalization strategies as well. In a recent publication, we hypothesized that each surface texturing represents a so-called 'turnover point', which distinguishes between positive and negative cell responses [14]. This turnover point has to be cell specific. We demonstrated that this turnover point was dependent on good or poor attachment of fibroblasts [14]. Surface impact on neuronal differentiation was verified with respect to the differentiation of PC-12 cell line cultured on nanostructures in Pt [18]. As PC-12 cells are suspension cells, the impact of additional coatings with LA, COL, PDL, and a combination of COL and PDL was further investigated. Nanostructuring significantly enhanced cell attachment classified by FAK p-Tyr^{397}, which is only expressed in the cells when they are bound to the surface via integrin receptors (figure 5) [19]. Cell differentiation was dependent on the surface design and culturing conditions using NGF-free or -containing cell culture medium. Without NGF, no differentiation was possible as shown for the neuronal markers beta III tubulin, formation of dendrites, MAP2 and synaptophysin (figure 5) [18]. This means that the attachment of the cells was not sufficient to stimulate neuronal differentiation. Predifferentiated PC-12 cells maintained their neuronal properties being in contact with the surfaces [18]. With the addition of NGF, undifferentiated PC-12 cells could differentiate on the structures directly (figure 5). The best extent of differentiation occurred on the surfaces that also showed the highest extent of FAK p-Tyr^{397}. This was the case for nanostructures, when they were combined with coating. However, coatings of LA or PDL were not sufficient [18].

Which mechanisms are responsible for this specific and selective cell guidance are poorly understood. However, this knowledge is essential to understand and explain the observed cell responses. Moreover, being able to characterize the basic differences of competitive cells beforehand could facilitate finding appropriate biomaterial interface properties for selective cell guidance. To get more insights, biomaterial–cell interactions have to be addressed in general. In the first place, components of the ECM adsorb to the material surface. This process basically depends on electrostatic interactions, van der Waals forces, time, interaction area, protein–surface distances, competitive adhesive proteins and others [19]. Then, several components of the ECM can build up a linkage between the material surface and cells and serve as adhesion ligands, which directly bind to integrin receptors within the cell membrane. Well-described adhesion ligands are LA, FIB, collagens or vitronectin, which can further be divided into several subgroups [4,29,30]. Integrins are transmembrane receptors, which always consist of one α and one β subunit [31]. Before connecting to a specific binding motif of each adhesion ligand, for example RGD sequences of FIB, integrins are activated via inside-out signalling cascades using the cytoskeletal molecule talin [32–35]. There is an overlap in specificity, with many integrins being able to bind several ligands; additionally, one cell type can express a large variety of integrins [4].

As soon as ECM adhesion ligands are connected to integrins, small dot-like focal complexes are formed followed by mature focal contacts with clustered integrins. On the one hand, this process stabilizes cell-binding to the surface via the additional recruitment of other cytoskeletal elements [36,37]. On the other hand, the now-formed focal adhesion complex initiates outside-in signalling cascades, which depend on many different components [4,38]. These interactions have an impact on cell migration but also stimulate transcription factors within the nucleus, which then control survival, proliferation, intercellular communication and differentiation. Additionally, the functionality of transcription factors is dependent on growth factors.

Cell specificity of these processes is not only very probable, but also extremely difficult to address owing to the complexity and large variety of molecules involved.

To get more insights, we started investigating the role of ECM components. In table 1, it is shown that in comparison to LA, FIB significantly enhanced the adhesion time, cell length and doubling time of fibroblasts. Neuroblastoma cells responded best to LA. A cell-specific ligand priority ranking was confirmed elsewhere [4]. This finding might be the first key to explain the topographical control of fibroblasts versus neuroblastoma cells: it can be supposed that the surface texturing negatively affects the adsorption of the fibroblast-specific adhesion ligand FIB, while the adsorption of the neuroblastoma-specific adhesion ligand LA is not negatively affected. As surface structuring increases the entire surface area, it is unlikely that the adsorbed density of the ligands was reduced. It is rather related to changes in the ligand conformation on the structured topography [19]. We recently demonstrated that functional FIB with a freely available RGD-binding sequence was less presented on microsized spike structures in silicone [14]. That the conformation of FIB is very sensitive to the properties of the biomaterial interface was also demonstrated for unstructured materials with different wettabilities [39,40]. For instance, we have shown that FIB adsorbs better to flat hydrophilic surfaces than to hydrophobic ones [19]. The conformation of LA or in other words the availability of integrin-binding fragments of LA, which differ from the RGD-binding sequence in FIB, was probably not negatively affected by the topography. Further studies are necessary to confirm this thesis.

Afterwards, the role of integrins needs to be characterized. Owing to the described overlap in binding possibilities of ligands and integrins and the fact that cells express several functional integrin heterodimers, more basic details on that topic are hard to find. Some studies found that the integrin spacing within the cell membrane and functional clustering was dependent on the spacing of possible anchorage points on the surface [41]. However, this spacing was set in the nanometre range. Therefore, the impact of microsized texturing is not known so far and requires further analysis.

The topographical influence on cell morphology and the organization of the cytoskeleton is presented in figure 2.

In what manner this topographical-induced event guides the molecular signalling cascades in detail cannot be answered so far. Anyway, a correlation between mechanical events and biochemical signalling, on the one hand, and intracellular forces on stem cell differentiation, on the other hand, are well known [42,43]. In this connection, more general information on physiological events referring to cell–cell contacts and intercellular communication is necessary. A correlation between intercellular communication and ECM components plus morphology and apoptotic reactions has recently been reported [4,44].

The analysis of neuronal differentiation of PC-12 cells pointed out that a successful and even significantly enhanced attachment of the cells was not sufficient to stimulate neuronal differentiation (figure 5) [18]. This is in accordance with the general description of biomaterial–cell interaction, as the functionality of transcription factors also requires the addition of growth factors. However, under appropriate cell culture conditions substrates with the best cell adhesion also stimulated the best cell differentiation. Therefore, innovative functionalization strategies of biomaterials should always take the attachment of cells and their corresponding growth factors into account.

5. Conclusion

A topographical functionalization of biomaterial surfaces is a promising approach to optimize tissue responses and to reduce biological reactions like inflammation when tissues are in contact with the biomaterial and by this means enhances implant integration and functions. From the technical point of view, femtosecond laser ablation enables a great flexibility to structure solid materials in a very precise, controllable and reproducible manner. Thereby, material surface properties can specifically be improved, *inter alia* electrochemical properties. From the biological point of view, this technique offers a good platform to study systematically the interaction with cells within a defined nano- or microsized environment. The formation of fibrotic scar tissue can significantly be inhibited *in vitro* by appropriate surface texturing, while neuronal attachment and differentiation can be enhanced simultaneously. This selective cell control correlates with cell-specific differences in cell adhesion mechanisms, the key event to induce cell behaviour via outside-in signalling cascades, which in turn are selectively affected by the biomaterial interface. Knowledge about these biomaterial–cell interactions is crucial for the development of innovative and effective functionalization strategies needed for all biomedical applications.

Acknowledgements. The authors thank Prof. Dr A. Ngezahayo (Institute of Biophysics, Leibniz University Hannover, Germany) for granting the use of the fluorescence microscope.

Funding statement. This work was partly supported by German Research Foundation Cluster of Excellence Rebirth 'From Regenerative Biology to Reconstructive Therapy', DFG SFB599 'Sustainable Bioresorbing and Permanent Implants of Metallic and Ceramic Materials' and by BMBF project REMEDIS.

References

1. Anderson JM. 2001 Biological responses to biomaterials. *Annu. Rev. Mater. Res.* **31**, 81–110. (doi:10.1146/annurev.matsci.31.1.81)
2. Babensee JM, Anderson JM, McIntire LV, Mikos AG. 1998 Host response to tissue engineered devices. *Adv. Drug Del. Rev.* **33**, 111–139. (doi:10.1016/S0169-409X(98)00023-4)
3. Frantz C, Stewart KM, Weaver VM. 2011 The extracellular matrix at a glance. *J. Cell Sci.* **123**, 4195–4200. (doi:10.1242/jcs.023820)
4. Schlie-Wolter S, Ngezahayo A, Chichkov B. 2013 The selective role of ECM components of cell adhesion, morphology, proliferation and communication in vitro. *Exp. Cell Res.* **319**, 1553–1561. (doi:10.1016/j.yexcr.2013.03.016)
5. Giancotti FG, Ruoslahti E. 1999 Integrin signalling. *Science* **285**, 1028–1032. (doi:10.1126/science.285.5430.1028)
6. Curtis A, Wilkinson C. 2001 Nantotechniques and approaches in biotechnology. *Trends Biotechnol.* **19**, 97–101. (doi:10.1016/S0167-7799(00)01536-5)
7. Flemming RG, Murphy CJ, Abrams GA, Goodman SL, Nealey PF. 1999 Effects of synthetic micro- and nano-structured surfaces on cell behaviour. *Biomaterials* **20**, 572–588. (doi:10.1016/S0142-9612(98)00209-9)
8. Wilkinson CDW, Riehle M, Wood M, Gallagher J, Curtis ASG. 2002 The use of materials patterned on a nano- and micro-metric scale in cellular engineering. *Mater. Sci. Eng. C* **19**, 263–269. (doi:10.1016/S0928-4931(01)00396-4)
9. Bettinger CJ, Langer R, Borenstein JT. 2009 Engeneering substrate micro- and nanotopography to control cell functions. *Angew. Chem. Int. Ed. Engl.* **48**, 5406–5414. (doi:10.1002/anie.200805179)
10. Schlie S, Fadeeva E, Koroleva A, Ovsianikov A, Koch J, Ngezahayo A, Chichkov BN. 2011 Laser-based nanoengineering of surface topographies for biomedical applications. *Photonics Nanostruct.* **9**, 159–162. (doi:10.1016/j.photonics.2010.09.006)
11. Gaggl A, Schultes G, Müller W, Kärcher H. 2000 Scanning electron microscopical analysis of laser-treated titanium implant surfaces: a comparative study. *Biomaterials* **21**, 1067–1073. (doi:10.1016/S0142-9612(00)00002-8)
12. Petö G, Karacs A, Pászti Z, Guczi L, Divinyi T, Joób A. 2002 Surface treatment of screw shaped titanium dental implants by high intensity laser pulses. *Appl. Surf. Sci.* **186**, 7–13. (doi:10.1016/S0169-4332(01)00769-3)
13. Chichkov B, Momma C, Nolte S, Alvensleben F, Tunnermann A. 1996 Femtosecond, picosecond and nanosecond laser ablation of solids. *Appl. Phys.* **63**, 109–115. (doi:10.1007/BF01567637)
14. Schlie S, Fadeeva E, Koch J, Ngezahayo A, Chichkov BN. 2010 Femtosecond laser fabricated spike structures for selective control of cellular behaviour. *J. Biomater. Appl.* **25**, 217–233. (doi:10.1177/0885328209345553)
15. Fadeeva E, Schlie S, Koch J, Chichkov BN. 2010 Selective cell control provided by surface structuring for orthopedic applications. *J. Adhes. Sci. Technol.* **24**, 2257–2270. (doi:10.1163/016942410X508000)
16. Fadeeva E, Schlie S, Koch J, Chichkov BN, Vorobyev AY, Guo C. 2009 Femtosecond laser-induced surface structures on platinum and their effects on surface wettability and fibroblast cell proliferation. In *Contact angle, wettability and adhesion*, vol. 6 (ed. KL Mittal), pp. 163–171. Boca Raton, FL: CRC Press.
17. Schlie S, Fadeeva E, Koroleva A, Chichkov BN. 2012 Laser-engineered topography: correlation between structure dimensions and cell control. *J. Mater. Sci. Mater. Med.* **23**, 2813–2819. (doi:10.1007/s10856-012-4737-9)
18. Schlie-Wolter S, Deiwick A, Fadeeva E, Paasche G, Lenarz T, Chichkov BN. 2013 Topography and coating of platinum improve the electrochemical properties and neuronal guidance. *Appl. Mater. Interfaces* **5**, 1070–1077. (doi:10.1021/am3028487)
19. Schlie S, Gruene M, Dittmar H, Chichkov B. 2012 Dynamics of cell attachment: adhesion time and force. *Tissue Eng. C* **18**, 688–696. (doi:10.1089/ten.tec.2011.0635)
20. Fadeeva E, Schlie S, Koch J, Ngezahayo A, Chichkov BN. 2009 The hydrophobic properties of femtosecond laser fabricated spike structures and

their effects on cell proliferation. *Phys. Status Solidi A* **6**, 1348–1351. (doi:10.1002/pssa.200881063)

21. Lee J, Cuddihy MJ, Kotov NA. 2008 Three-dimensional cell culture matrices: state of art. *Tissue Eng. B* **14**, 61–86. (doi:10.1089/teb.2007.0150)
22. Koroleva A, Schlie S, Fadeeva E, Gittard SD, Miller P, Ovsianikov A, Koch J, Narayan RJ, Chichkov BN. 2010 Microreplication of laser-fabricated surface and three-dimensional structures. *J. Opt.* **12**, 124009. (doi:10.1088/2040-8978/12/12/124009)
23. Wenzel RN. 1936 Resistance of solid surfaces to wetting by water. *Ind. Eng. Chem.* **28**, 988–994. (doi:10.1021/ie50320a024)
24. Cassie ABD, Baxter S. 1944 Wettability of porous surfaces. *Trans. Faraday Soc.* **40**, 546–551. (doi:10.1039/tf9444000546)
25. Cogan SF. 2008 Neural stimulation and recording electrodes. *Annu. Rev. Biomed. Eng.* **10**, 275–309. (doi:10.1146/annurev.bioeng.10.061807.160518)
26. Kovacs GTA. 1994 Introduction to the theory, design, and modeling of thin film microdevices for neural interfaces. In *Enabling technologies for cultured neural networks* (eds DA Stenger, TM McKenna), pp. 121–165. New York, NY: Academic Press.
27. Stieglitz T. 2004 Electrode materials for recording and stimulation. In *Neuroprosthetics theory and practice*, vol. 2 (eds KW Horch, GS Dhillon), pp. 475–516. Singapore: World Scientific Publishing Co.
28. Schlie S, Koroleva A, Fadeeva E, Chichkov B. 2011 Control of fibroblasts by micro-sized surface topographies. In *Proc. 2nd Int. Conf. on Tissue Engineering, Lisbon, Portugal, 2–4 June 2011* (eds PR Fernandes, PJ Bártolo, J Folgado, HC Rodrigues, RB Ruben, H Almeida, MR Dias), pp. 51–55. Hamilton, Canada: IST Press.
29. Tzu J, Marinkovich MP. 2008 Bridging structure with function: structural, regulatory, and developmental role of laminins. *Int. J. Biochem. Cell Biol.* **40**, 199–214. (doi:10.1016/j.biocel.2007.07.015)
30. Heino J, Huhtala M, Käpylä J, Johnson MS. 2009 Evolution of collagen-based adhesion systems. *Int. J. Biochem. Cell Biol.* **41**, 341–348. (doi:10.1016/j.biocel.2008.08.021)
31. Gahmberg CG, Fagerholm SC, Nurmi SM, Chavakis T, Marchesan S, Grönholm M. 2006 Regulation of integrin activity and signalling. *Biochim. Biophys. Acta* **1790**, 431–444. (doi:10.1016/j.bbagen.2009.03.007)
32. Hynes RO. 2002 Integrins: bidirectional, allosteric signaling machines. *Cell* **110**, 673–687. (doi:10.1016/S0092-8674(02)00971-6)
33. Anthis NJ, Campbell ID. 2011 The tail of integrin activation. *Trends Biochem. Sci.* **36**, 191–198. (doi:10.1016/j.tibs.2010.11.002)
34. Arnaout MA, Goodman D, Xiong J-P. 2007 Structure and mechanics of integrin-based cell adhesion. *Curr. Opin. Cell Biol.* **19**, 495–507. (doi:10.1016/j.ceb.2007.08.002)
35. Sonnenberg A, Linders CJT, Modderman PW, Damsky CH, Aumailley M, Timpl R. 1990 Integrin recognition of different cell-binding fragments of laminin (P1, E3, E8) and evidence that $\alpha 6\beta 1$ but not $\alpha 6\beta 4$ functions as a major receptor for fragment E8. *J. Cell Biol.* **110**, 2145–2155. (doi:10.1083/jcb.110.6.2145)
36. Geiger B, Bershadsky A. 2001 Assembly and mechanosensory function of focal contacts. *Curr. Opin. Cell Biol.* **13**, 584–592. (doi:10.1016/S0955-0674(00)00255-6)
37. Wozniak MA, Modzelewska K, Kwong L, Keely PJ. 2004 Focal adhesion regulation of cell behaviour. *Biochim. Biophys. Acta* **1692**, 103–119. (doi:10.1016/j.bbamcr.2004.04.007)
38. Lo SH. 2006 Focal adhesions: what's new inside. *Dev. Biol.* **294**, 280–291. (doi:10.1016/j.ydbio.2006.03.029)
39. García AJ, Boettiger D. 1999 Integrin–fibronectin interactions at the cell–material interface: initial integrin binding and signalling. *Biomaterials* **20**, 2427–2433. (doi:10.1016/S0142-9612(99)00170-2)
40. Baujard-Lamotte L, Noinville S, Goubard F, Marque P, Pauthe E. 2008 Kinetics and conformational changes of fibronectin adsorbed onto model surfaces. *Colloids Surf. B* **63**, 129–137. (doi:10.1016/j.colsurfb.2007.11.015)
41. Cavalcanti-Adam EA, Volberg T, Micoulet A, Kessler H, Geiger B, Spatz JP. 2007 Cell spreading and focal adhesion dynamics are regulated by spacing of integrin ligands. *Biophys. J.* **92**, 2964–2974. (doi:10.1529/biophysj.106.089730)
42. Ingber DE. 2003 Tensegrity I. Cell structure and hierarchical systems biology. *J. Cell Sci.* **116**, 1157–1173. (doi:10.1242/jcs.00359)
43. Kelly DJ, Jacobs CR. 2010 The role of mechanical signals in regulating chondrogenesis and osteogenesis of mesenchymal stem cells. *Birth Defects Res. C Embryo Today* **90**, 75–85. (doi:10.1002/bdrc.20173)
44. Schlie S, Mazur K, Bintig W, Ngezahayo A. 2010 Cell cycle regulation of gap junction coupling and apoptosis in GFSHR-17 granulosa cells. *J. Biomed. Sci. Eng.* **3**, 884–891. (doi:10.4236/jbise.2010.39118)